

**Cell Reports, Volume 32**

**Supplemental Information**

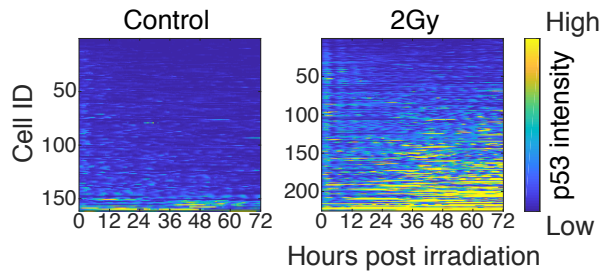
**A Switch in p53 Dynamics Marks Cells**

**That Escape from DSB-Induced Cell Cycle Arrest**

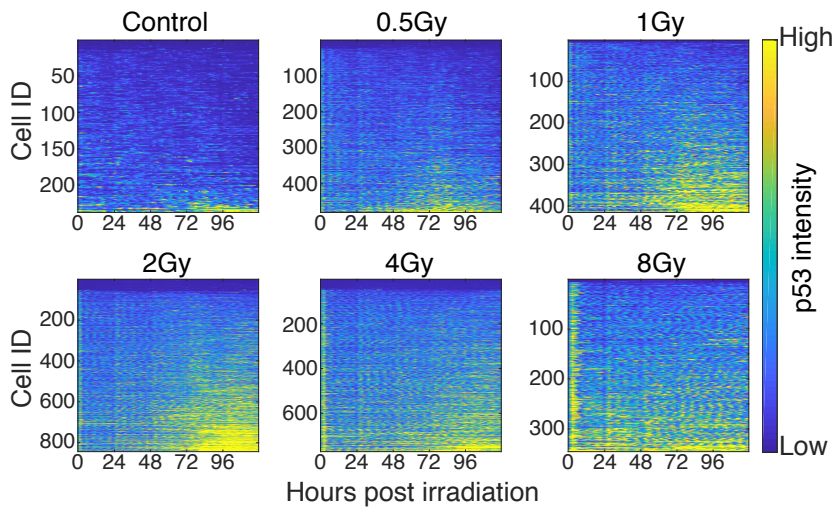
**Michael Tsabar, Caroline S. Mock, Veena Venkatachalam, Jose Reyes, Kyle W. Karhohs, Trudy G. Oliver, Aviv Regev, Ashwini Jambhekar, and Galit Lahav**

# Supplemental Figure 1

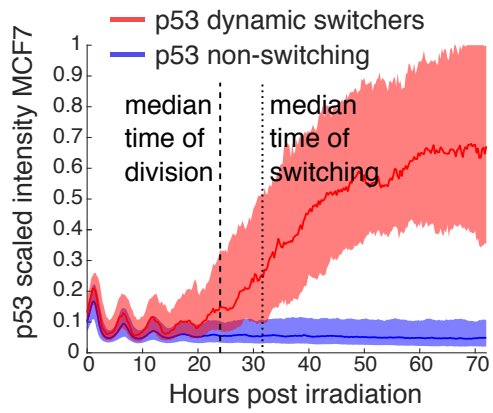
## A A549



## B RPE1



## C



## D

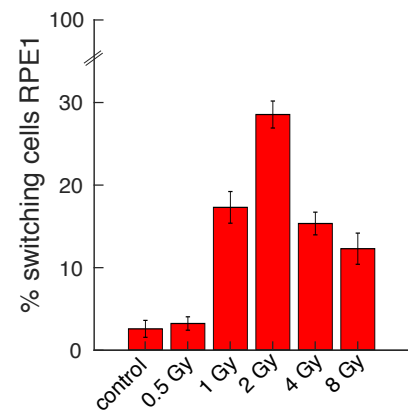


**Figure S1. Related to Figure 2.**

(A) Heatmap of p53-Neon-green fluorescence intensity in single A549 cells following 2Gy ionizing irradiation. Cells were tracked for 72 h (x-axis) and sorted by mean p53-intensity (y-axis). Each row on the y-axis represents a single cell. Fluorescence intensity is color coded from blue (low intensity) to yellow (high intensity).

(B) Heatmaps of p53-Venus fluorescence intensity in single RPE1 cells following increasing doses of irradiation, plotted as described in (A).

(C) Plot of scaled intensity of p53-Venus tracks from all irradiation doses clustered by k-means. Switching cluster in red, non-switching in blue. Shaded area represents the first to third quantile of each cluster, bolded line is the median signal.

(D) Percent switchers at different irradiation doses in RPE1 cells ( $n > 200$  for each radiation dose conditions) as determined by k-means clustering. Error bars represent standard error of the proportions.

Supplemental Figure 2

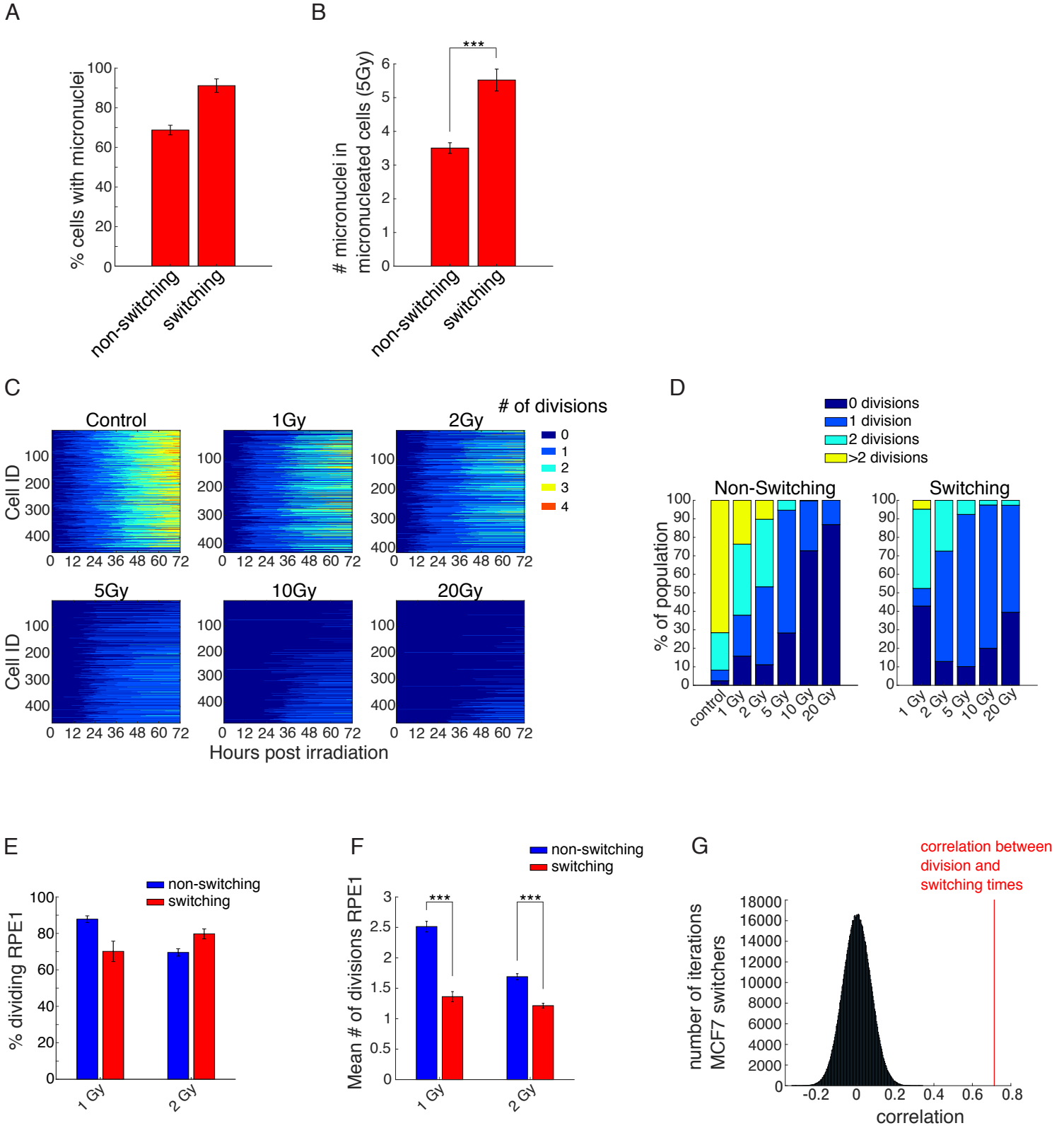


**Figure S2. Related to Figure 3.**

(A) Percentages of switching and non-switching MCF7 cells treated with 5 Gy irradiation that exhibit micronuclei. Error bars represent standard error of the proportions.

(B) Mean number of micronuclei in switching and non-switching MCF7 cells treated with 5 Gy irradiation and that have undergone division. Error bars represent standard error,  $p < 0.0005$ .

(C) Heatmaps of divisions at different doses of irradiation. Each row represents a cell, and cells are sorted by p53 intensity (data from Figure 2C). A change in color indicates a division event.

(D) Distribution of number of divisions at different irradiation doses in the switching and non-switching populations.

(E) Percent of RPE1 switching and non-switching cells treated with 1Gy and 2Gy irradiation that have undergone divisions. Error bars represent standard error of the proportions.

(F) Mean number of divisions in RPE1 switching and non-switching cells treated with 1 Gy or 2 Gy irradiation. Error bars represent standard error  $p < 0.0005$ .

(G) Distribution of the correlation between division times and switching times in randomized order (gray area) compared to the experimental correlation (red line) in MCF7 cells.

### Supplemental Figure 3

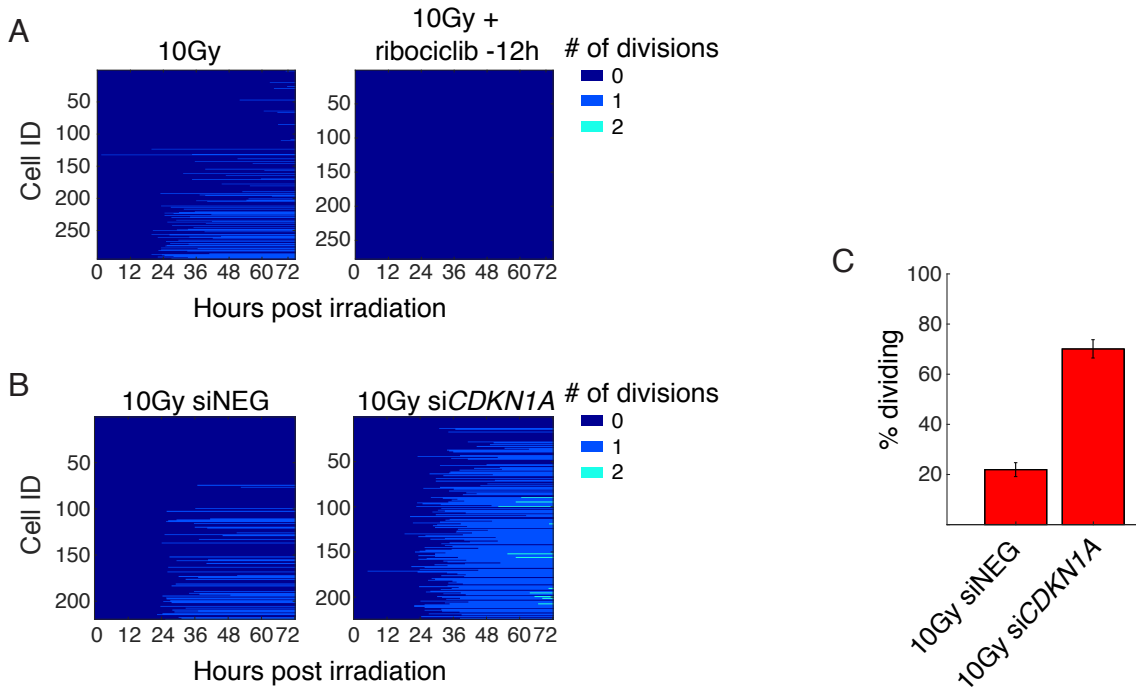


**Figure S3. Related to Figure 3.**

(A) Heatmaps of cell divisions following 10 Gy irradiation in control cells (left panel) and ribociclib treated cells (right panel) from Figure 3D.

(B) Heatmaps of divisions following 10 Gy irradiation in cells treated with control (right panel) or *CDKN1A* (p21, left panel) siRNA, from Figure 3E. siRNA was added 2 hr after irradiation.

(C) Bar graph of the percent of cells that divided at least once during the time course in control or *CDKN1A* siRNA-treated cells.



**Figure S4. Related to Figures 4 and 5.**

(A) ATR inhibitor (VE822, 50 nM) was added 20 hr following irradiation. CHK1 phosphorylation was used to test ATR activity.

(B) Levels of p53 at the indicated timepoints following 10 Gy irradiation of wild-type or *PIDD1* knock-out cells. Actin is shown as a loading control.

(C) p53 intensity in WT and *PIDD1* knock-out cells for 24 hr following 10 Gy irradiation, normalized to the p53 intensity prior to irradiation. Line represents median signal, shaded area represents 1<sup>st</sup> to 3<sup>rd</sup> quantiles.

(D) p53 levels following siRNA knockdown of *PIDD1*. Actin is shown as a loading control.

(E) *PIDD1* mRNA levels following 10 Gy irradiation in cells treated with control or *PIDD1* siRNA. *PIDD1* signal was normalized to *GAPDH* and compared to 0h siNEG.

(F) Mean number of micronuclei in dividing WT and *PIDD1* KO cells treated with 10 Gy. Error bars represent standard error,  $p > 0.05$ .

(G) Levels of Mdm2, its degradation product Mdm2-p60 (red arrow), and p53 in response to different concentrations of Caspase-2 inhibitor (Z-VDVAD-FMK). Actin is shown as a loading control.

(H) Heatmap of PIDD1-ECFP signal in uninduced cells (left panel) and after induction with doxycycline (right panel) from Figure 4C.

(I) Heatmap of divisions in the experiment detailed in Figure 5G.

# Supplemental Figure 5

A

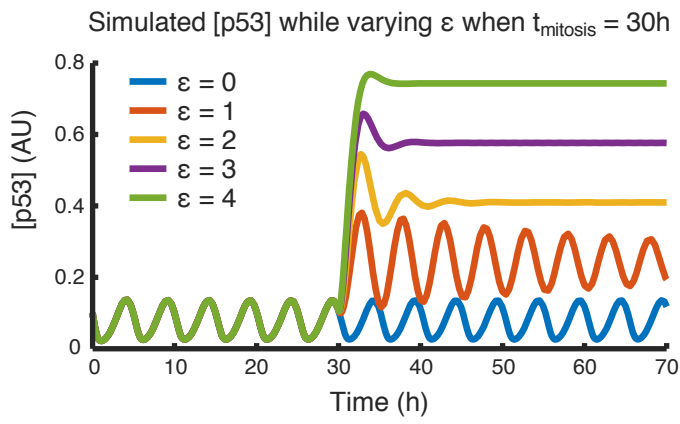


**Figure S5. Related to Figure 6**

Simulated p53 levels over time when running the computational model for values of  $\varepsilon$  (the post-mitotic PIDDosome-dependent MDM2 degradation rate) ranging from 0 to 4  $C_s^{-1} \cdot h^{-1}$ . Note that “switching” behavior is observed when  $\varepsilon$  exceeds a value of  $\sim 1 C_s^{-1} \cdot h^{-1}$ .  $C_s$  = simulated concentration units.

Supplemental Table 1

Parameter	Description	Value
$\alpha$	p53 production rate	$0.4 C_S \cdot h^{-1}$
$\beta$	Mdm2-dependent p53 degradation rate	$4 h^{-1}$
$\gamma$	Concentration for half-maximal p53 degradation	$0.01 C_S$
$\psi$	p53-dependent Mdm2 production rate	$0.6 h^{-1}$
$T_{del}$	Time delay in Mdm2 production	$0.7 h$
$\delta$	Mdm2 degradation rate	$0.4 h^{-1}$
$\varepsilon$	PIDDosome-dependent Mdm2 degradation rate	$0 C_S^{-1} \cdot h^{-1}$ to simulate no PIDDosome-dependent Mdm2 degradation. $3 C_S^{-1} \cdot h^{-1}$ to simulate PIDDosome-dependent Mdm2 degradation
$t_{mitosis}$	Time of mitosis	$30 h$
$[p53]_i$	Initial concentration of p53	$0.1 C_S$
$[Mdm2]_i$	Initial concentration of Mdm2	$0.15 C_S$
$[PIDDosome]$	Steady-state concentration of PIDDosome	$1 C_S$

### **Table S1. Related to Figure 6**

Parameters and initial conditions of the mathematical model used to generate Figure 6B.  $C_s$  = simulated concentration units. Parameters were set to the values published by Heltberg et al. (Heltberg et al., 2019), with the exception of  $\varepsilon$ , which is introduced here and was varied systematically (see Fig. S5) to select a value that recapitulates the observed p53 behavior. The time delay in MDM2 production was chosen to yield persistent oscillations, based on the limit cycle analysis of Heltberg et al. (Heltberg et al., 2019) and is consistent with the time delay of 0.7 hr used by Batchelor et al. (Batchelor et al., 2008).